Journal of Atomic, Molecular, Condensed Matter & Nano Physics
Vol. 7, No. 3, pp. 145–154, 2020
ISSN 2582-8215 (online)
Published by RGN Publications
DOI: 10.26713/jamcnp.v7i3.1539

http://www.rgnpublications.com

Proceedings of ICACTCE'21
High School of Technology, Moulay Ismail University Meknes, Morocco, and
Faculty of Sciences and Techniques Mohammedia, Hassan II University, Morocco
March 24 – 26, 2021, Morocco
Editors**:** Mariyam Ouaissa, Mariya Ouaissa, Sarah El Himer, and Zakaria Boulouard

Research Article

Synthesis and Characterization of Cu-Doped SnO_2 ($Sn_{0.98}Cu_{0.02}O_2$) Thin Film by Sol-gel Technique for LPG Sensing

Bouabida Seddik *[1], Benkara Salima[1], Ghamri Houda[2] and Fares Abdelhakim[1]

[1] *Department of Electrical Engineering, Larbi Ben M'hidi University, Oum El Bouaghi, Algeria*
[2] *Department of Physic, Hadj Lakhder University, Batna, Algeria*

Abstract. In this study Cu-doped SnO_2 ($Sn_{0.98}Cu_{0.02}O_2$) thin film was deposited on the glass substrate by sol-gel dip-coating technique. The structural, morphological, and optical properties of the prepared film were studied by *X-ray diffraction* (XRD), *Optical Microscopy* (OM), and Uv-visible spectroscopy respectively. XRD analysis revealed that the structure of our deposited film is hexagonal and the crystallite size is found to be 3.89 nm. The surface morphological studied by (OM) indicates that the film is homogeneous. The result of optical properties shows high transmittance estimated at 73.98% and the optical band gap was found 3.961 eV. The gas sensing properties of the prepared film were examined at different operating temperatures and different volume concentrations of *liquefied petroleum gas* (LPG). It was found that Cu doped SnO_2 has an excellent response and recovery time for 1.8 vol% LPG at 250 °C, their values are equal to 11s and 19s respectively, obtained sensors presents high selectivity to LPG against H_2S, NH_3 and CO_2.

Keywords. SnO_2 thin film; LPG sensing; Sol-gel; Reducing gas; Response

PACS. 67.80.dm; 07.07.Df; 68.55.-a; 61.05.cp

1. Introduction

Metal oxide semiconductors (MOS) are promising for gas sensing applications because of their high sensitivity, low fabrication cost [5], Among the (MOS), tin dioxide (SnO_2) is one

*Corresponding author: bouabida.seddik@univ-oeb.dz

of the compound semiconductors of n-type, with a wide band gap of 3.6 eV, large excition binding energy of 130 meV [7], and excellent optical and electrical properties. Due to their low fabrication cost, SnO_2 thin films have a large number of technological applications including a variety of sensors for instance gas sensors [1, 4, 17], optical sensors [6], and solar cells [24]. SnO_2 nanostructures had been discovered in various forms such as SnO_2 thin film [10], *nanowires* (NWs) [12], nanorods [2], nanorings [13], and nanotubes [19]. To develop efficient gas sensors, SnO_2 thin film has been modified by doping with metallic impurities which is a promising way as it modifies the electronic properties of film and the gas molecule adsorption sites which in turn affect the sensing properties [9, 16, 21]. Therefore, SnO_2 thin film that was doped by Cu has resulted in enhancing the LPG sensing performance [15, 20]. In the literature, many studies about the response of SnO_2 thin films used as a gas sensor towards various harmful gases such as H_2S, CO, CO_2, and LPG [1, 8, 20, 23]. Among these gases, *Liquid petroleum gas* (LPG) is widely used in industry and in domestic utilization as a source of energy. It is a combustible gas composed mainly of butane and propane. It is very dangerous due to the explosion caused by a leak [20]. Hence, it is crucial to detect it.

In the present work, we report the process for the preparation of Cu doped SnO_2 thin film, from [$SnCl_2 \cdot 2H_2O$] and [$CuCl_2 \cdot 2H_2O$] solution using the sol-gel dip-coating method. *X-ray diffraction* (XRD), *Optical Microscopy* (OM), and Uv-visible spectroscopy are exploited to study structural, morphological, and optical properties of Cu doped SnO_2 thin film and their LPG sensing properties.

The rest of this paper is organized as follows. In Section 2 experimental materials and methods are exposed. In Section 3 gas sensing results is discussed. The conclusion and future works are given in Section 4.

2. Experimental Materials and Methods

2.1 Materials

As a starting material, tin (II) Chloride dihydrate [($SnCl_2 \cdot 2H_2O$), (Merck, $\geq 98\%$)] was used. Ethanol [(C_2H_6O), (purity $\geq 99.8\%$, Sigma Aldrich)] and Triethanolamine [(TEA, $C_6H_{15}NO_3$, (purity $\geq 98\%$, Sigma Aldrich)] were used as a solvent and stabilizer, respectively. The dopant source of copper was Copper (II) chloride dihydrate [($CuCl_2 \cdot 2H_2O$), (Merck, $\geq 98\%$)]. All reagents were used without further purification.

2.2 Preparation of Cu-doped SnO_2 Solution

Tin (II) Chloride dihydrate (2.030g), and dopant Copper (II) chloride dihydrate (0.057g) at concentration ratio 2% were dissolved into 30 ml of absolute ethanol at room temperature, which corresponds to a molar concentration of 0.3 M with magnetic stirring at 70 °C. Then a volume of 1.22 ml of TEA is added with a pipette which corresponds to the molar ratio equal to 1. It is noted directly after the addition of the TEA that the coloration of the solution becomes clear. The solution was stirred at 70 °C for 1 h 30 min to yield a clear and homogeneous solution; which served as a coating solution after cooling to room temperature as shown in Figure 1. The coating was usually made 24 h after the solution was prepared, so it will become more stable.

Figure 1. Image of prepared solution Cu doped SnO_2

2.3 Preparation of Cu-doped SnO_2 Film

In the formation of thin film from the prepared gel, a microscope slide was used as the substrate. For this, the slides prepared in the dimensions of 5 cm × 2.5 cm were ultrasonically cleaned with ethanol and acetone for 10 min, respectively, followed by rinsing with deionized water. After the cleaning process was completed, the glass substrates were finally dried at 70 °C for 30 min.

The cleaned glass substrate was immersed in the prepared solution and withdrawn at the rate of 60 mm/min. The deposited films were then dried at 200 °C for 10 min and finally annealed at a temperature of 500 °C for 60 min. The procedures from coating to drying were repeated 15 times.

2.4 Characterization and Gas Sensing Measurements

The crystallinity of SnO_2 film was measured using an X-ray diffractometer Equinox 100 with CuKα (λ = 1.54059 Å) radiation. The image was captured by optical microscope model euromex (ME2660-2665) with camera euromex CMEX5000. The Optical properties of the film were studied using Jasko V-750 visible spectrophotometer. The sensing performance of the synthesized Cu doped SnO_2 film was investigated. For measurement of the electrical resistance by two Ag electrodes printed on the surface.

The sensing element was kept directly on contact with a heater inside the gas chamber in a temperature range which varies from 150 °C to 300 °C. The electrical resistance of the sensing element was measured before (R_a) and after exposure to LPG (R_g) using a digital multimeter linked to personal computer. LPG (reducing gas) response% presented in term $[(R_a - R_g)/R_a] \times 100$.

3. Results and Discussion

3.1 X-ray Diffraction Analysis

Figure 2 shown XRD patterns of $Sn_{0.98}Cu_{0.02}O_2$ film after 1 h of annealing at 500 °C. All peaks at angles (2θ) of 26.681°; 33.856°; 37.976°; 51.885° and 65.913° correspond to (110), (101), (200), (211), and (301) planes respectively, with preferential orientation in (110) direction. The observed peaks are well indexed to the tetragonal phase of SnO_2 which are in good agreement with JCPDS data card 41-1445.

No extra peak corresponding to Cu or any other impurity such as metallic Sn or other oxide phases of SnO and CuO were detected confirming a good dilution of the Cu atoms in the SnO_2 structure.

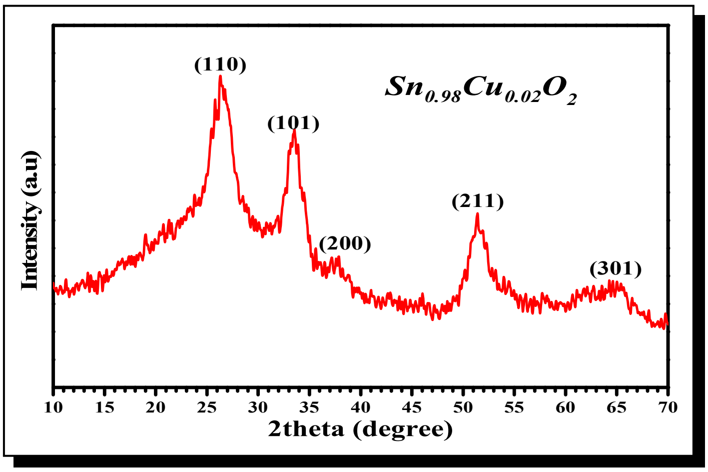

Figure 2. X-ray diffraction spectra of Cu doped SnO_2 thin film

The size crystallite of ZnO in (110) orientation is calculated from the Scherrer equation (3.1), using XRD results [3]:

$$D = \frac{0.9\lambda}{\beta\cos\theta}, \tag{3.1}$$

where 0.9 is the shape factor, λ is the x-ray wavelength, β is the full width at half maximum of the peak in radian, and θ is the Bragg angle. The value of size crystallite Cu doped SnO_2 ($Sn_{0.98}Cu_{0.02}O_2$) is 3.89 nm.

The lattice constants ($a = b$ and c) were calculated by the relation between inter-planar spacing (d) and Miller indices (hkl) from eq. (3.2) [11]:

$$\frac{1}{d^2} = [(h^2 + k^2)/a^2] + [l^2/c^2]. \tag{3.2}$$

The dislocation density (δ) defined as the length of dislocation lines per unit volume of the crystal, and was calculated from D using eq. (3.3) [11]:

$$\delta = \frac{1}{D^2}. \tag{3.3}$$

The Lattice strain (ε) is given by eq. (3.4) [11]:

$$\varepsilon = \frac{\beta\cos\theta}{4}. \tag{3.4}$$

The crystallinity parameters are summarized in Table 1.

Table 1. Crystallinity parameters of $Sn_{0.98}Cu_{0.02}O_2$ thin film

Cu doping (wt.%)	Lattice constant		Crystallite size (D)(nm)	Dislocation density (δ) ($\times 10^{14}$ lines/m^2)	Lattice strain (ε)
	($a = b$)(nm)	(c)(nm)			
2	0.4789	0.3262	3.89	660.846	0.0089

3.2 Optical Microscopy Analysis

Figure 3 shows the image captured by optical microscopy (X1000 magnification); this image reveals that the structure depicts a profile of a homogeneous and dense surface.

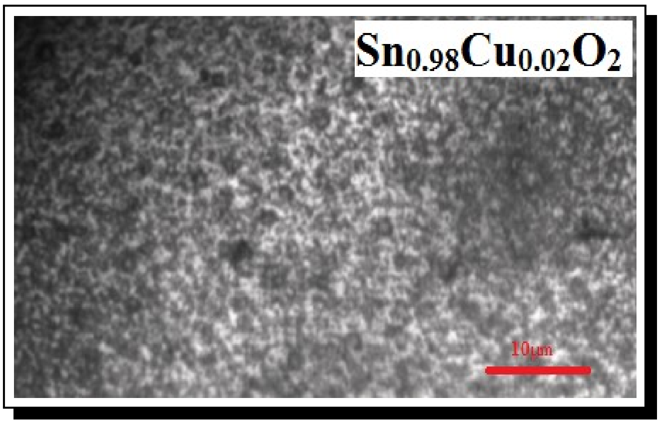

Figure 3. Optical image of Cu doped SnO_2 thin film

3.3 Optical Analysis

The optical transmission spectrum of Cu doped SnO_2 ($Sn_{0.98}Cu_{0.02}O_2$) thin film was shown in Figure 4. The curve reveals that the film has an abrupt absorption edge near 380 nm and shows a high optical transmission of about 73, 98%.

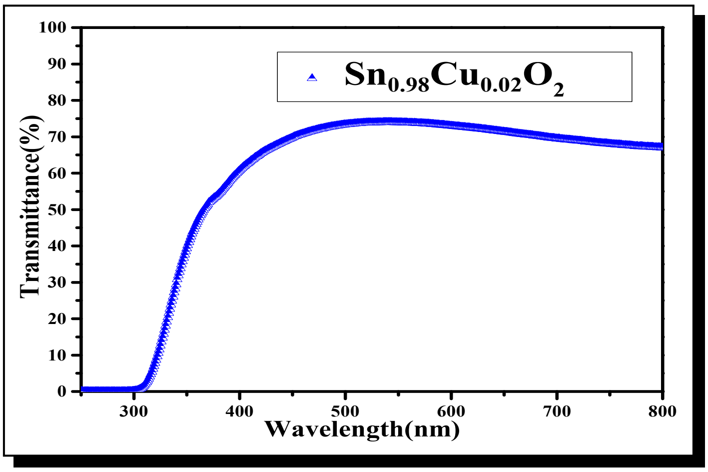

Figure 4. Transmittance curve of Cu doped SnO_2 thin film

The optical band gap energy (E_g) of the film can be obtained by plotting $(\alpha h\nu)^2$ verses $h\nu$ and extrapolating the straight-line portion of this plot to the energy axis as shown in Figure 5. The photon energy at the point where $(\alpha h\nu)^2$ is zero is bandgap energy ($E_g = 3.961$ eV) [22].

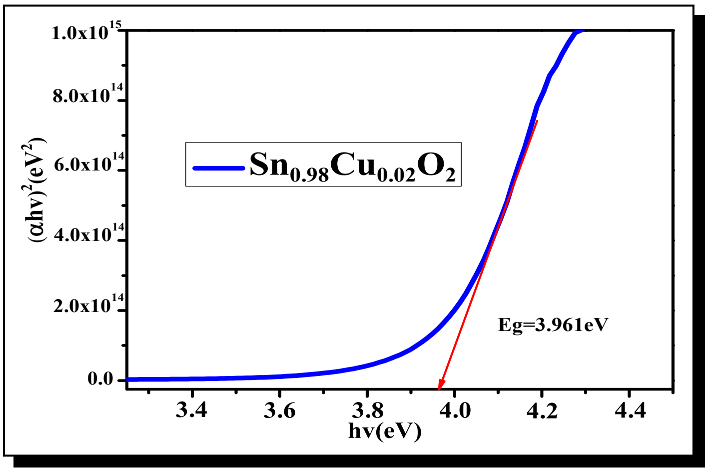

Figure 5. Variation of $(\alpha h\nu)^2$ versus $h\nu$ for Cu doped SnO_2 thin film

3.4 Gas Sensing Analysis

The LPG (reducing gas) sensing mechanism in the case of n-type SnO_2 semiconductor is depicted in Figure 6. When the Cu doped SnO_2 film is exposed to air, atmospheric oxygen molecules get adsorbed on the surface of the film in the form of ionic species i.e. oxygen ions O_2^- (ads) and O^- (ads) depending on operating temperatures by capturing electrons from the conduction band of SnO_2 following the given equations:

$$O_{2(\mathrm{ads})} + e^-_{(SN_2\,\mathrm{surface})} \leftrightarrow O^-_{2(\mathrm{ads})} \qquad [T < 100\,^\circ C], \tag{3.5}$$

$$O_{2(\mathrm{ads})} + e^-_{(SN_2\,\mathrm{surface})} \leftrightarrow 2O^-_{2(\mathrm{ads})} \qquad [100\,^\circ C < T < 300\,^\circ C]. \tag{3.6}$$

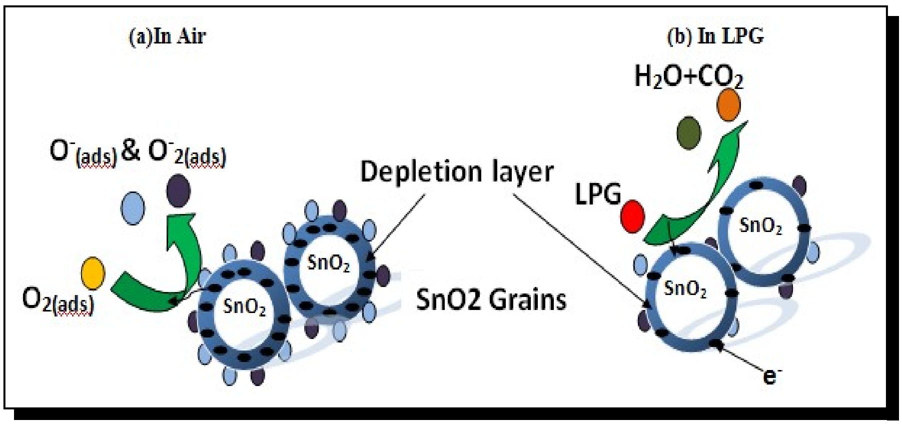

Figure 6. Schematic of sensing mechanism (a) In air; (b) In liquefied petroleum gas (LPG)

When the sample exposed to air, oxygen ions get adsorbed on the surface of Cu doped SnO_2 by capturing electrons, there is a formation of a depletion region of large width, where the electrical resistance of the sample increases as shown in Figure 6(a). But upon exposure to LPG (reducing gas), these oxygen ionic species react with LPG forming CO_2 and H_2O as shown in eqs. (3.7) and (3.8) [18], The electrons returned to the Cu doped SnO_2 surface resulting in a decrease in the width of the depletion region and hence a decrease in electrical resistance [14] as shown in Figure 6(b).

$$C_nH_{2n+2} + 2O^-_{(ads)} \xrightarrow{150°\text{-}300\,°C} C_nH_{2n} : O + H_2O + e^-, \tag{3.7}$$

$$C_nH_{2n} : O + O^-_{(ads)} \xrightarrow{150°\text{-}300\,°C} CO_2 + H_2O + e^-, \tag{3.8}$$

where C_nH_{2n+2} represents different hydrocarbons (mixture of butane and propane).

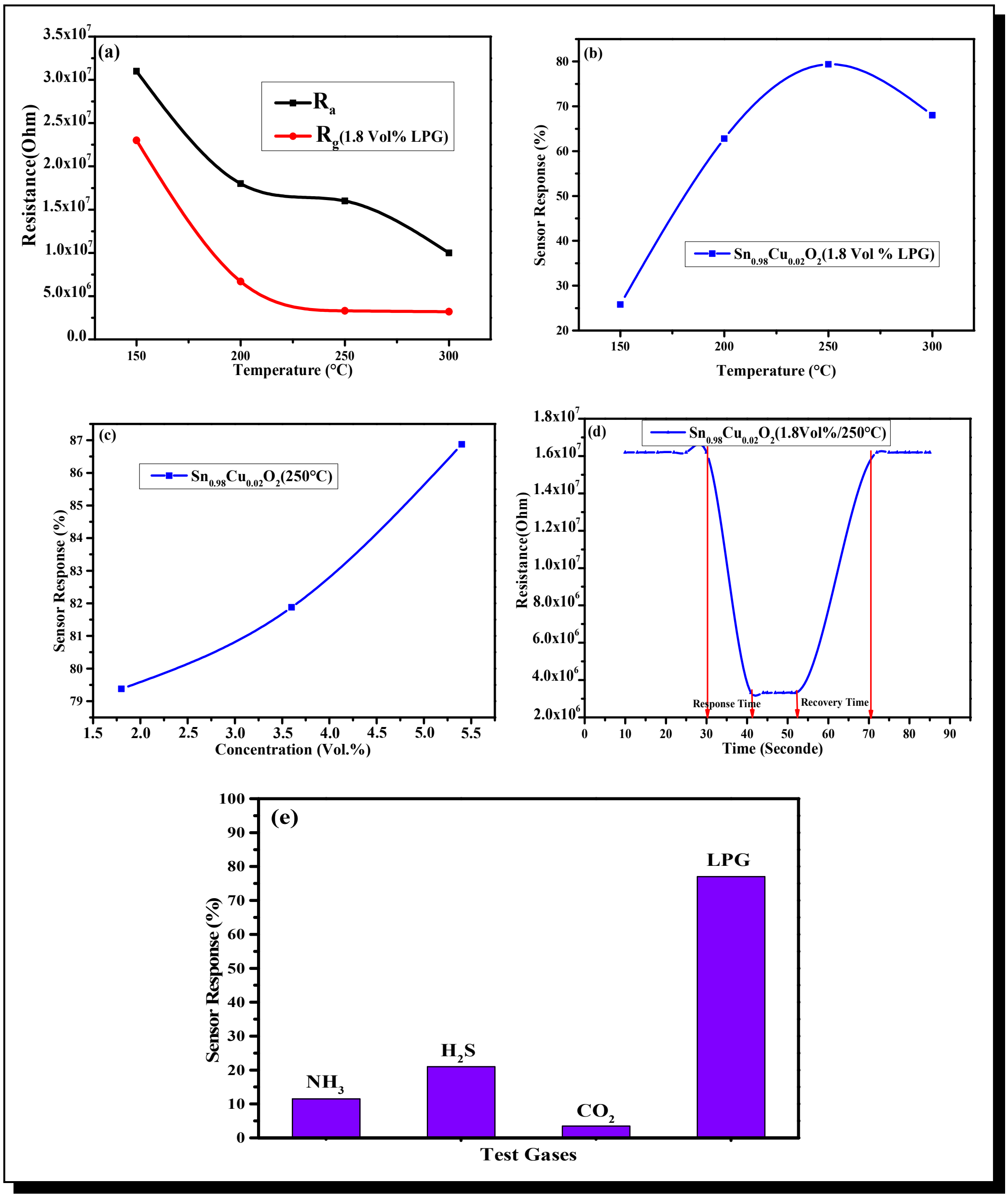

Figure 7. (a) Variation resistances R_a and R_g with operating temperatures, (b) Sensor response vs temperature (1.8 Vol%LPG), (c) Sensor response vs LPG Vol % (@250 °C), (d) Response and recovery times (1.8 Vol%LPG@250°C), (e) Selectivity study of Cu doped SnO_2 thin film at 250°C

Figure 7(a) shows the variation of resistance in the air (R_a) and resistance in the presence of LPG (R_g) and Figure 7(b) shows the sensing response of Cu doped SnO_2 for 1.8 Vol % LPG at different operating temperatures in the range of 150-300 °C. As can be clearly seen the sensor response increased with temperature up to 250 °C beyond which is decreased and hence the operating temperature is fixed at 250 °C. Figure 7(c) shows the variation in the sensor response with LPG concentration at the operating temperature of 250 °C, it can be seen that the sensor response increases with the increase in the concentration of LPG. This is attributed to the dense surface coverage of the sample with the LPG gas molecules. Figure 7(d) shows the response-recovery plot of the 2% Cu doped SnO_2 at an operating temperature of 250°C towards 1.8 Vol % of LPG gas. Initially, the 2%Cu doped SnO_2 sensor shows a stable resistance of 16 MΩ which instantaneously drops to 3.3 MΩ in about 11 sec (response time). When the LPG is vacuumed from the chamber the resistance starts increasing again to the initial value in about 19 sec (recovery time).

The selectivity of the sample was also investigated in this work. Figure 7(e) shows the sensor responses of 2% Cu doped SnO_2 towards different gases such as H_2S, NH_3, and CO_2 with 1.8 Vol % concentrations at an operating temperature of 250 °C. As can be seen from Figure 7(e) sensor prepared using 2% Cu doped SnO_2 exhibits a higher response for LPG among the test gases which clearly demonstrates the selective nature of the sensor.

4. Conclusion

In this paper, we have synthesized Cu doped SnO_2 ($Sn_{0.98}$ $Cu_{0.02}O_2$) by sol-gel dip-coating technique and investigated their structural, morphological, optical, and gas sensing properties. The maximum sensitivity to LPG showed at 250 °C. The correspondent response time is about 11 seconds and recovery time is around a third of a minute. The high sensitivity to LPG may be attributed to low thickness (approximately 0.54 μm), low crystallite dimension (approximately 3.89 nm calculated using Scherrer equation), and porosity. The excellent selectivity for LPG with negligible interference from CO_2 making them very promising for LPG gas sensing applications. Our future works will oriented towards reducing operating temperature, and improving sensors selectivity.

Acknowledgement

The authors are thankful to the Laboratory of Active Components and Materials, Larbi Ben M'hidi University, Oum El Bouaghi, Algeria for their help in synthesis, characterization, and gas sensing studies.

Competing Interests

The authors declare that they have no competing interests.

Authors' Contributions

All the authors contributed significantly in writing this article. The authors read and approved the final manuscript.

References

[1] N. Bhardwaj, A. Pandey, B. Satpati, M. Tomar, V. Gupta and S. Mohapatra, Enhanced CO gas sensing properties of Cu doped SnO_2 nanostructures prepared by a facile wet chemical method, *Physical Chemistry Chemical Physics* **28** (2016), 18846 – 18854, DOI: 10.1039/C6CP01758D.

[2] A. Bouaine, N. Brihi, G. Schmerber, C.U. Bouillet, S. Colis and A. Dinia, Structural, optical, and magnetic properties of co-doped SnO_2 powders synthesized by the coprecipitation technique, *The Journal of Physical Chemistry C* **111** (2007), 2924 – 2928, DOI: 10.1021/jp066897p.

[3] P. Chetri, B. Saikia and A. Choudhury, Structural and optical properties of Cu doped SnO_2 nanoparticles: an experimental and density functional study, *Journal of Applied Physics* **113** (2013), 233514, DOI: 10.1063/1.4811374.

[4] S. Das and V. Jayaraman, SnO_2: a comprehensive review on structures and gas sensors, *Progress in Materials Science* **66** (2014), 112 – 255, DOI: 10.1016/j.pmatsci.2014.06.003.

[5] A. Dey, Semiconductor metal oxide gas sensors: a review, *Materials Science & Engineering B* **229** (2018), 206 – 217, DOI: 10.1016/j.mseb.2017.12.036.

[6] E.A. Floriano, L.V.A. Scalvi, J.R. Sambrano and A. Andrade, Decay of photo-induced conductivity in Sb-doped SnO_2 thin films, using monochromatic light of about bandgap energy, *Applied Surface Science* **267** (2013), 164 – 168, DOI: 10.1016/j.apsusc.2012.09.003.

[7] K. Godinho, A. Walsh and G. Watson, Energetic and electronic structure analysis of intrinsic defects in SnO_2, *The Journal of Physical Chemistry C* **113** (2009), 439 – 448, DOI: 10.1021/jp807753t.

[8] K.C. Hsu, T.H. Fang, Y.J. Hsiao and C.A. Chan, Highly response CO_2 gas sensor based on Au-La_2O_3 doped SnO_2 nanofibers, *Materials Letters* **261** (2020), 127144, DOI: 10.1016/j.matlet.2019.127144.

[9] K. Jain, R.P. Pant and S.T. Lakshmikumar, Effect of Ni doping on thick film SnO_2 gas sensor, *Sensors and Actuators B: Chemical* **113** (2005), 823 – 829, DOI: 10.1016/j.snb.2005.03.104.

[10] I.H. Kadhim, H.A. Hassan and F.T. Ibrahim, Hydrogen gas sensing based on nanocrystalline SnO_2 thin films operating at low temperatures, *International Journal of Hydrogen Energy* **45** (2020), 25599 – 25607, DOI: 10.1016/j.ijhydene.2020.06.136.

[11] S.T. Khlayboonme and W. Thowladdab, Synthesis and characterization of Cu-doped SnO_2 thin films by aerosol pyrolysis technique for gas sensor application, *Key Engineering Materials* **766** (2018), 205 – 210, DOI: 10.4028/www.scientific.net/KEM.766.205.

[12] V. Kumar, S. Sen, K.P. Muthe, N.K. Gaur, S.K. Gupta and J.V. Yakhmi, Copper doped SnO_2 nanowires as highly sensitive H_2S gas sensor, *Sensors and Actuators B* **138** (2009), 587 – 590, DOI: 10.1016/j.snb.2009.02.053.

[13] S.H. Li, Z. Chu, F.F. Meng, T. Luo, X.Y. Hu, S.Z. Huang and Z. Jin, Highly sensitive gas sensor based on SnO_2 nanorings for detection of isopropanol, *Journal of Alloys and Compounds* **688** (2016), 712 – 717, DOI: 10.1016/j.jallcom.2016.07.248.

[14] L. Mei, Y. Chen and J. Ma, Gas sensing of SnO_2 nanocrystals revisited: developing ultra-sensitive sensors for detecting the H_2S leakage of biogas, *Scientific Reports* **4** (2014), 6028, DOI: 10.1038/srep06028.

[15] S.E. Mirsalary and E.S. Iranizad, The effect of Cu doping on LPG response of the SnO_2 nanostructure layer, *Advanced Materials Research* **829** (2013), 391 – 395, DOI: 10.4028/www.scientific.net/AMR.829.391.

[16] S. Nagirnyak and T. Dontsova, Effect of modification/doping on gas sensing properties of SnO_2, *Nano Research & Applications* **3** (2017), 8 pages, DOI: 10.21767/2471-9838.100025.

[17] I.S. Naji, Characterization of CuO-doped tin dioxide thin films prepared by pulsed-laser deposition for gas-sensing applications, Nanomaterials, *Proceedings of the Institution of Mechanical Engineers, Part N: Journal of Nanomaterials, Nanoengineering and Nanosystems* **233** (2018), 17 – 25, DOI: 10.1177/2397791418819267.

[18] S.S. Nkosi, I. Kortidis, D.E. Motaung, R.E. Kroon, N. Leshabane, J. Tshilongo and O.M. Ndwandwe, The effect of stabilized ZnO nanostructures green luminescence towards LPG sensing capabilities, *Materials Chemistry and Physics* **242** (2020), 122452, DOI: 10.1016/j.matchemphys.2019.122452.

[19] K.R. Park, H.B. Cho, J. Lee, Y. Song, W.B. Ki and Y.H. Choa, Design of highly porous SnO_2-CuO nanotubes for enhancing H_2S gas sensor performance, *Sensors and Actuators B: Chemical* **302** (2020), 127179, DOI: 10.1016/j.snb.2019.127179.

[20] D. Patil, V. Patil and P. Patil, Highly sensitive and selective LPG sensor based on α-Fe_2O_3 nanorods, *Sensors and Actuators B: Chemical* **152** (2011), 299 – 306, DOI: 10.1016/j.snb.2010.12.025.

[21] A. Salehi and M. Gholizade, Gas-sensing properties of indium-doped SnO_2 thin films with variation in indium concentration, *Sensors and Actuators B: Chemical* **89** (2003), 173 – 179, DOI: 10.1016/S0925-4005(02)00460-4.

[22] A. Tombak, Y.S. Ocak and F. Bayansal, Cu/SnO_2 gas sensor fabricated by ultrasonic spray pyrolysis for effective detection of carbon monoxide, *Applied Surface Science* **493** (2019), 1075 – 1082, DOI: 10.1016/j.apsusc.2019.07.087.

[23] W. Wei, Y. Dai and B. Huang, Role of Cu doping in SnO_2 sensing properties toward H_2S, *The Journal of Physical Chemistry C* **115** (2011), 18597 – 18602, DOI: 10.1021/jp204170j.

[24] A.J. Yun, J. Kim, T. Hwang and B. Park, Origins of efficient Perovskite solar cells with low-temperature processed SnO_2 electron transport layer, *ACS Applied Energy Materials* **2** (2019), 3554 – 3560, DOI: 10.1021/acsaem.9b00293.